Direct measurement of the $\bar{K}N \to \pi\Sigma$ scattering amplitude below the $\bar{K}N$ threshold employing the $d(K^-, N)"\pi\Sigma"$ reaction

Kentaro Inoue

February 1, 2025

Contents

1 Introduction **3**
- 1.1 $\Lambda(1405)$ and $\bar{K}N$ interaction 3
- 1.2 $d(K^-, n)$ reaction 6
- 1.3 The J-PARC E31 experiment 7

2 Experimental setup **12**

3 Analysis **13**

4 Discussion **14**
- 4.1 Decomposition of the $K^- d \to n\pi^+\pi^- n$ events 14
  - 4.1.1 Backward $\pi^\mp\Sigma^\pm$ event selection 14
  - 4.1.2 Template fitting 14
- 4.2 Conversion to the cross section 14
- 4.3 Spectra 14
  - 4.3.1 Qualitative properties of obtained spectra 14
  - 4.3.2 Comparison with theoritical calculations 14
  - 4.3.3 $\bar{K}N$ Pole parameters assuming the 2-step reaction . . 14
  - 4.3.4 Comparison with DCC model 14

5 Conclusion **15**

A $\pi^0\Sigma^0$ spectrum analysis **16**

B Detector resolution **17**
- B.1 CDC resolution 17
- B.2 Detector resolution on the $d(K^-, N)$ 17

C $d(K^-, n)K^0 n$ analysis **18**

Chapter 1

Introduction

1.1 $\Lambda(1405)$ and $\bar{K}N$ interaction

The $\Lambda(1405)$ is a hyperon with strangeness $S = -1$, isospin $I = 0$ and spin and spin parity $J^P = (\frac{1}{2})^-$. In the latest Particle Data Group (PDG) [1], the mass and the width of the $\Lambda(1405)$ are assigned to $1405.1^{+1.3}_{-1.0}$MeV and 50.5 ± 2.0MeV respectively, based on several papers [2–4].

The existence of the $\Lambda(1405)$ was predicted for the first time by R. H. Dalitz and S. F. Taun in 1959 as a quasi-bound state of $\bar{K}N$ [5]. The candidate was reported to have been found in the $K^-p \to \pi\pi\pi\Sigma$ reaction at the Lawrence Radiation Laboratory in 1961 [6]. The excess was reported in the neutral $\pi\Sigma$ spectrum, $K^-p \to \pi^\pm\pi^\mp(\pi\Sigma)^0$, in the $\Lambda(1405)$ region compared to the doubly charged spectrum, $K^-p \to \pi^+\pi^+(\pi^-\Sigma^-)$ or $K^-p \to \pi^-\pi^-(\pi^+\Sigma^+)$, in this paper. However, there was not enough statistical data to discuss lineshape. There was also the problem of ambiguity about where each π came from.

In order to solve these problems, R. J. Hemingwey reported high-statistics $\pi^+\Sigma^-$ and $\pi^-\Sigma^+$ spectra using the $K^-p \to \pi^-\Sigma^+(1660) \to \pi^-\pi^+(\pi^\mp\Sigma^\pm)$ with 4.2 GeV/c K^- beam [7]. In these spectra, the momentum transfer was restricted to, $t(K^-, \pi^-)$ <1.0 GeV/c, in order to increase the purity of $\Sigma^+(1660)$. As a result, the $\Sigma^+ \to \pi^0 p$ decay event of the $K^-p \to \pi^-\Sigma^+(1660) \to \pi^-\pi^+(\pi^-\Sigma^+)$ reaction gave a $\pi^-\Sigma^+$ spectrum with almost no background. R. H. Dalitz and A. Deloff obtained the mass and width of the $\Lambda(1405)$ as 1406.4 ± 4.0 MeV and 50 ± 2 MeV [2] by adapting the M-matrix method to this spectrum, and these parameters were adopted for the PDG. On the other hand, the $\pi^+\Sigma^-$ spectrum of the $K^-p \to \pi^-\Sigma^+(1660) \to \pi^-\pi^+(\pi^+\Sigma^-)$ reaction had a background due to the ambiguity of the origin

of the π^-.

Considering the $\Lambda(1405)$ as a $\bar{K}N$ bound state, the $\bar{K}N$ interaction should be attractive. From the 1960's to the 1980's, various $K^-p \to$ meson-baryon, e.g., K^-p, K^0n, $\pi\Lambda$, $\pi\Sigma$, and so on, scattering data were measured on hydrogen target using bubble chambers to study the $\bar{K}N$ interaction [8–12]. This method of course did not allow access below the $\bar{K}N$ threshold and measurements in the low energy region were difficult and data were not enough. Nevertheless, the value of the $\bar{K}N$ interaction at the $\bar{K}N$ threshold was obtained by exterior it from the high energy region, where there is abundant data, using several models [13–15]. Due to the lack of data in the low energy region, these values varied. However, they were all attractive and consistent with the $\Lambda(1405)$ being a $\bar{K}N$ bound state.

A direct measurement of the $\bar{K}N$ interaction at the $\bar{K}N$ threshold was attempted by binding a K^- meson to a hydrogen atom instead of an electron and measuring the characteristic X-ray shift. Around 1980, experiments with liquid hydrogen reported a positive shift, implying that the $\bar{K}N$ interaction is repulsive [16–18]. This result was inconsistent with $\bar{K}N$ scattering experiments, which regarded the $\bar{K}N$ interaction as an attractive force.

Iwasaki et al. pointed out that these experiments showed a poor signal-to-noise ratio in the region of interest where the energy shift is below zero. To remedy this problem, they performed an experiment using a gaseous hydrogen target at KEK-PS [19] and found a negative energy shift peak and concluded that the $I = 0$ $\bar{K}N$ interaction is attractive. The experiment was updated to high precision by the SHIDDARTA collaboration [20] and its values were used as constraints to extrapolate $\bar{K}N$ scattering amplitudes below the $\bar{K}N$ threshold from $\bar{K}N$ scattering experiments.

The conclusion that the $\bar{K}N$ interaction is attractive accelerated theoretical analyses that consider the $\Lambda(1405)$ as a $\bar{K}N$ bound state. In this framework, the $\Lambda(1405)$ is considered to be dynamically generated and decays to $\pi\Sigma$ via the $\bar{K}N$ channel. In this depiction, the Lagrangian includes strange sector with $\bar{K}N$, $\pi\Lambda$, $\pi\Sigma$, $\eta\Lambda$, $\eta\Sigma$, and $K\Xi$ channels is used. The low-energy perturbation expansion of this Lagrangian was considered difficult to analysis near the $\Lambda(1405)$ region. Therefore, the chiral unitary model was proposed to extend the effective region near the $\Lambda(1405)$ by imposing unitary conditions on mult-channels in the strangeness sector, and a theoretical analysis was proceeded using this model.

J. C. Nacher et al. [21] calculated $\pi\Sigma$ channels, i.e. $\pi^+\Sigma^-$, $\pi^0\Sigma^0$ and $\pi^-\Sigma^+$ line shapes from photoproduction, $\gamma p \to K^+\Lambda(1405)$, using the chiral unitary model. They showed that the $\pi\Sigma$ spectra differs depending on the charge mode and argued that the difference reflects the nature of $\Lambda(1405)$.

This suggests that not only the $I = 0$ $\bar{K}N$ interaction but also the $I = 1$ $\bar{K}N$ interaction affects the $\pi\Sigma$ spectra.

M. Niiyama et al. experimentally measured $\pi^+\Sigma^-$ and $\pi^-\Sigma^+$ spectra caused by photoproduction at LEPS [22]. They measured $\gamma p \to K^+(\pi^\pm\Sigma^\mp)$ spectra by detecting forward-scattered K^+ at $0.8 < \theta_{K^+}$ using a γ-ray beam of E_γ =1.5-2.4 GeV. They reported differences in their spectra below the $\bar{K}N$ threshold and showed the presence of $I = 0$ and $I = 1$ interference terms in Λ(1405). The CLAS collaboration reported spectra of all three $\pi\Sigma$ channels, with high statistical data on photoproduction [23, 24]. They measured the forward-scattered K^+, $0.6 < \Theta_{K^+} < 0.9$, using a γ-ray beam of $E_\gamma = 1.61$-1.91 GeV. The spectra show large differences at vicinity of the Λ(1405), suggesting more strongly the presence of $I = 1$ and interference term effects in this region. Although this spectra did not agree with the calculations by J.C.Nacher et. al. [21], it was shown by S.X.Nakamura and D.Jido that the spectra is reproduced by a gauge-invariant photoproduction mechanism using a chiral unitary model in which many parameters are introduced [25]. The fact that many parameters are introduced here means that the reaction mechanism is complex and there is interference of $I = 0$ and $I = 1$ between some parameters.

D.Jido et al. proposed that Λ(1405) is influenced by two poles strongly coupled to $\bar{K}N$ and $\pi\Sigma$, respectively, through a detailed theoretical analysis using the chiral unitary model [26]. According to this depiction, the $\bar{K}N$ pole appears above the conventional 1.405 GeV and the $\pi\Sigma$ pole appears below 1405MeV. The HADES collaboration performed Λ(1405) production experiments using *pp* collisions, a different reaction mechanism to photoproduction [27]. They reported $(\pi^\pm\Sigma^\mp)$ spectra from the $pp \to K^+p(\pi^\pm\Sigma^\mp)$ reaction using a proton beam with an energy of 3.5 GeV. The peak of the spectrum clearly appeared below 1.4 GeV. Thus, it was found that the spectrum of Λ(1405) depends on the reaction mechanism and the $\pi\Sigma$ channel, which reinforces the depiction that Λ(1405) is a dynamically generated meson baryon state and promots analysis according to this depiction.

Y. Ikeda et al. [28] and Z.-H. Geo et al. [29] improved the analysis of the chiral unitary model by constraining the $\bar{K}N$ interaction at the $\bar{K}N$ threshold from the X-ray shift by SHIDDARTA and reported the scattering amplitude for the $\bar{K}N$ interaction and the parameters for the Λ(1405). M. Mai et al. analysed in a similar way and obtained several solutions. Finally, they reporting two parameters for the Λ(1405) and the scattering amplitude for the $\bar{K}N$ interaction by sieving by $\pi\Sigma$ spectra by CLAS photoproduction [30].

For the higher energy regions, detailed partial-wave analyses have been

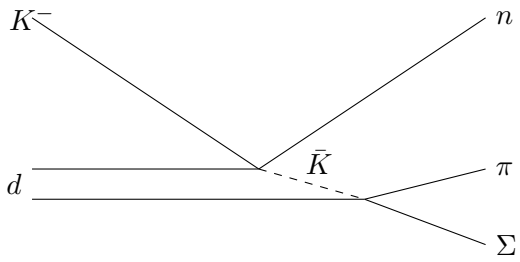

Figure 1.1: The diagram of 2step $K^- d \to n\pi\Sigma$ reaction.

carried out because of the large amount of scattering data available, as mentioned above, and many excited states of hyperons have been predicted, and many of them have been experimentally confirmed. The most recent static partial wave analysis was performed by a group at Kent State University (KSU) [31, 32]. However, in that analysis, $\Lambda(1405)$ was fixed to the value by PDG and the structure of $\Lambda(1405)$ could not be discussed. Kamano et al. reported the results of analysing the structure of dynamically generated $\Lambda(1405)$ by adapting the Dynamical Coupled Channel method, which extends partial wave analysis to dynamics, to strange sectors containing such as K, Λ, Σ and so on [33]. Although there were two DCC models due to shortage of data in the low momentum region, both models had two $I = 0$ poles below the $\bar{K}N$ threshold as in the chiral unitary model, with the higher pole strongly coupled to $\bar{K}N$ and the lower pole to $\pi\Sigma$. However, the position and width of these poles differed significantly between the two models.

1.2 $d(K^-, n)$ reaction

As mentioned above, $\Lambda(1405)$ is closely related to the $\bar{K}N$ interaction and scattering data below the $\bar{K}N$ threshold of Kaon and nucleon are desired, but cannot be scattered directly in free space due to energy conservation laws. By using a deuterium target, the irradiated Kaon beam is scattered by one nucleon, which energises the nucleon and becomes a virtual $\bar{K}$. The virtual $\bar{K}$ reacts with the residual nucleon and becomes $\pi\Sigma$. The diagram of this reaction is shown in Figure 1.1. By flying the virtual $\bar{K}$ to intermediate states, information below the $\bar{K}N$ threshold can be accessed.

An experiment to measure the πY spectrum from Y^* produced by irradiating liquid deuterium with a K^- beam at a momentum of 686-848 MeV/c

was performed at CERN by Braun et al. by a bubble chamber [34]. They only reported $K^-d \to n(\pi^+\Sigma^-)$ spectra as information containing $I = 0$. They also reported another pure $I = 1$ spectrum, $K^-d \to p(\pi^-\Lambda)$. It is well known that the p-wave scattering, $\Sigma(1385)$, is present in the $I = 1$ channel below the $\bar{K}N$ threshold. They estimated the influence of $\Sigma(1385)$ from the $\pi^-\Lambda$ spectrum and confirmed that its effect on the $\pi^+\Sigma^-$ spectrum is small.

The peak position of the $\pi^+\Sigma^-$ spectrum was clearly located in a region higher than the conventional 1405 MeV. Jido et al. showed that if this reaction is considered within the framework of the chiral unitary model, the influence of the $\bar{K}N$ poles is dominant and the peak position is around 1420 MeV, reproducing the experimental spectrum of $K^-d \to n(\pi^+\Sigma^-)$ [35]. In the same framework, Yamagata et al. calculated an $I = 1$ $\pi^-\Lambda$ spectrum incorporating $\Sigma(1385)$ and confirmed that it reproduced the experimental spectrum [36]. They estimated the influence of $\Sigma(1385)$ in the framework of this theoretical calculation and confirmed that the influence on the $\pi^+\Sigma^-$ spectrum was small.

However, they did not report a $\pi^-\Sigma^+$ spectrum and therefore could not discuss the influence of $I = 0$ and $I = 1$ interference on this reaction. They were also unable to discuss detailed kinematic factors because of the low momentum of the K^- beam and all the angles of the scattered nucleons were summarised.

The J-PARC E31 experiment was planned and performed to solve these problems [37]. The next subsection provides an overview of the J-PARC E31 experiment and the physics discussed in this paper.

1.3 The J-PARC E31 experiment

In the J-PARC E31 experiment, a liquid deuterium target is irradiated with a 1.0 GeV/c K^- beam to measure kinetics, which are identified by detecting super-forward scattered nucleons $\theta_n = 0$ degree. In this kinematics, the virtual $\bar{K}$ is recoiled backwards and reacts with residual nucleons to become $\pi\Sigma$. The mass of $\pi\Sigma$ is measured by the $d(K^-, N)$ missing mass method and the charge state of $\pi\Sigma$ is identified by measuring charged particles due to decay in a cylindrical detector system (CDS) placed around a liquid deuterium target.

After the J-PARC E31 experiment was proposed, a spectrum was calculated for the kinematics of the experiment based on several theories. It was argued by K. Miyagawa et al. [38] that $\Lambda(1405)$ is due to $\bar{K}N$ scattering in the low energy region and data from that region should be used for

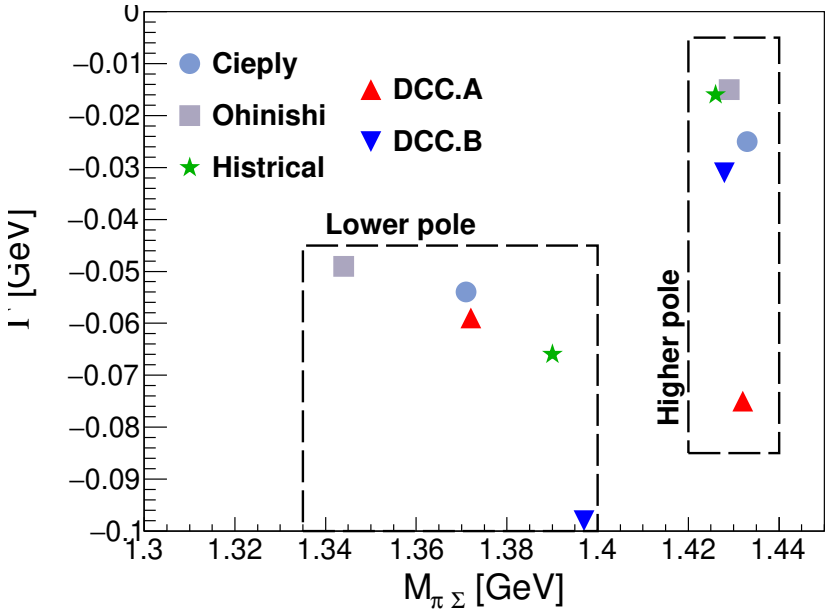

Figure 1.2: This figure shows the pole structure with $I = 0$ $\bar{K}N$ scattering amplitudes below the $\bar{K}N$ threshold used in the theoretical calculation of the predicted spectrum of the E31 experiment.

the second step scattering, while the J-PARC E31 experiment uses a high momentum K^- beam of 1.0 GeV/c, so $\bar{K}N$ scattering data from the high energy region should be used. They used scattering amplitudes from the partial wave analysis by the KSU group presented in Section 1.1 for the first scattering in the high energy region, and scattering amplitudes from the three chiral analyses for the $\bar{K}N$ scattering data in the low energy region of interest. One is from E. Oset et al. in the early period when chiral analysis was proposed [39], and the other two are from A. Cieplý et el. [40] and S. Ohinishi et el. [41] after the SIDDARTA result was presented. These two are imposed the constrain to the $\bar{K}N$ scattering amplitude by the $\bar{K}N$ scattering length from the kaonic hydrogen by SIDDARTA.

Also, theoretical spectra calculated by the DCC method introduced in Section 1.1 have also been reported by H. Kamano et al. [42]. The DCC method covers a wide region from the low-energy $\bar{K}N$ bound region of $\Lambda(1405)$ to the high-energy $\bar{K}N$ scattering of the first scattering of this reaction with continuous scattering amplitudes, which is used in this calculation. There are two models for the DCC method, both of which have two poles but their positions are significantly different.

The pole structure of the $I = 0$ poles below the $\bar{K}N$ threshold, i.e. $\Lambda(1405)$, used in these theoretical calculations is shown in Fig.1.2. All models have two poles, but their values vary widely from model to model.

Assuming a two-step reaction as described above, Noumi et. el. [43] focused on the second step of $\bar{K}N \to \pi\Sigma$ scattering and performed a fit using the scattering length and effective range, which are complex numbers, as free parameters. As a result, we obtained the values $A = [-1.12 \pm 0.11(fit)^{+0.10}_{-0.07}(syst.)] + [0.84 \pm 0.12(fit)^{+0.08}_{-0.07}(syst.)]$ fm and $R = [-0.18 \pm 0.32(fit)^{+0.08}_{-0.06}(syst.)] + [-0.40 \pm 0.13(fit) \pm 0.09(syst.)]$ fm for the scatter length and effective range resulting in Figure.1.3. From those values, the pole positon and width of $\Lambda(1405)$ are obtained as $1417.7^{+6.0}_{-7.4}(fit)^{+1.1}_{-1.0}(syst.)$ MeV/c^2 and $26.1^{+6.0}_{-7.9}(fit)^{+1.7}_{-2.0}(syst.)$ MeV/c^2. The scattering length and effective range are the first-order and second-order parameters in the low-energy expansion of the two-channel scattering between $\bar{K}N$ and $\pi\Sigma$. In that figure, the spectrum obtained from the experiment is depicted in the above panel, and the $\bar{K}N \to \bar{K}N$ scattering amplitudes for $I = 0$ obtained from the fit are depicted in the lower panel. In the above panel, the black error bars in the above figure are the spectra obtained from the $\Sigma^+\pi^-$ and $\Sigma^-\pi^+$ spectra with $I = 0$ and 1 and their interference terms, and the $\Sigma^-\pi^0$ spectrum with $I = 1$. The blue error bar is the $\Sigma^0\pi^0$ spectrum with $I = 0$. The spectra obtained from the fit are depicted by the red lines, where the

dashed lines do not include the detector resolution and the solid lines are convolved with the resolution. The estimation of the resolution is described in detail in Appendix.**??**. In the lower panel, the real and imaginary parts of the $\bar{K}N \to \bar{K}N$ scattering amplitude obtained from the fit are shown as black and red lines, respectively. The real and imaginary parts of the scattering amplitudes are represented by the black and red lines, respectively, in the down figure. The green and blue vertical lines represent the $\bar{K}N$ threshold and the pole position of $\Lambda(1405)$, respectively. These analyses are described in detail in Section.**??**.

In this paper, detailed measurements and analysis methods for the $\pi^-\Sigma^+$, $\pi^+\Sigma^-$, and $\pi^-\Sigma^0$ spectra measured in the J-PARC E31 experiment are explained. The $\pi^-\Sigma^+$ and $\pi^-\Sigma^-$ spectra have contributions from $I = 0$, $I = 1$, and their interference terms, while $\pi^-\Sigma^0$ only contributes from pure $I = 1$. From these three spectra, we discuss the respective contributions by decomposing them into $I = 0$, $I = 1$, and their interference terms, and comparing them with the spectra predicted from the theory introduced earlier. The $\pi^0\Sigma^0$ spectrum shown in Figure. 1.3 is described in detail in the paper by S. Kawasaki [44], and a summary is given in the Appendix A.

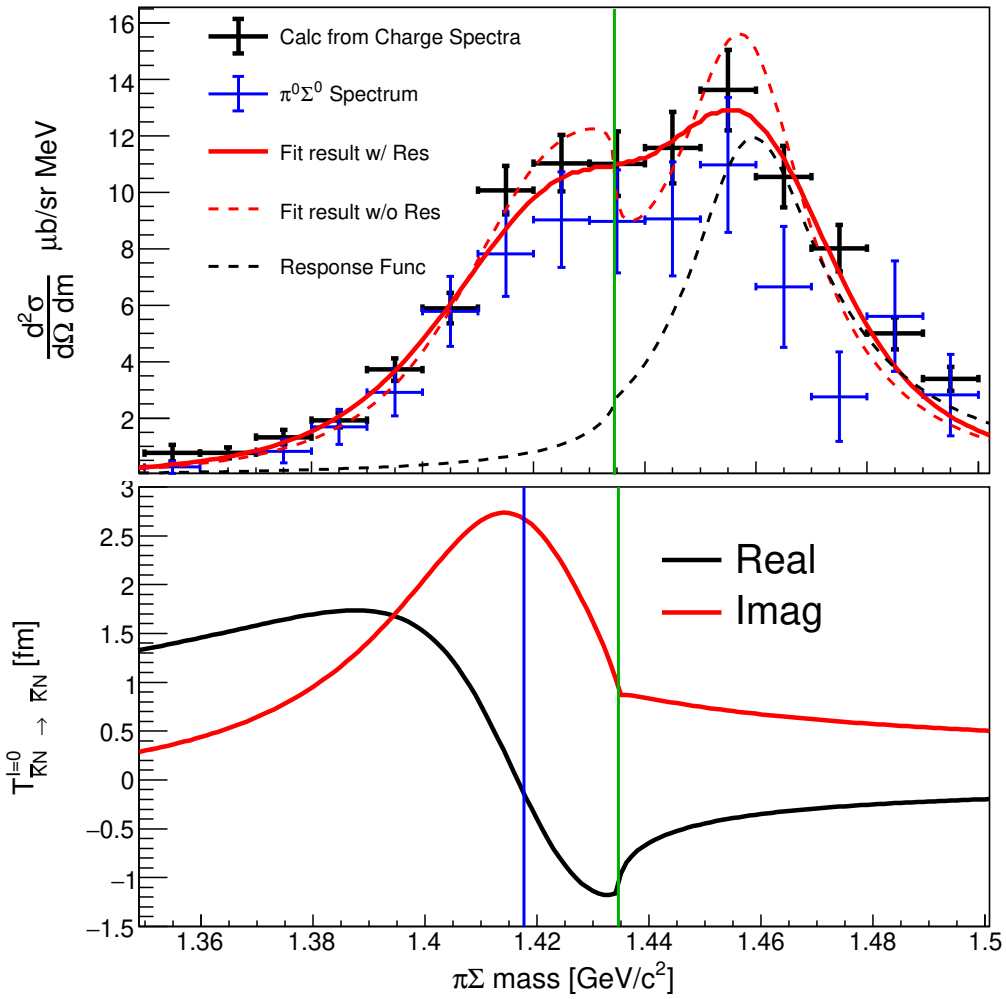

Figure 1.3: This picture shows the result of fitting the spectrum with E31 by Noumi et al []. The error bars in the upper panel represent experimental data, with black representing the $I = 0$ spectrum calculated from $\pi^-\Sigma^+$, $\pi^+\Sigma^-$ and $\pi^0\Sigma^-$, and blue representing the $\pi^0\Sigma^0$ spectrum with $I = 0$. The solid red line is the result of a fit assuming a two-step reaction, solid and dashed represents with and without detector resolution. The lower panels show the scattering amplitude of the second step $\bar{K}N \to \bar{K}N$ scattering obtained by the fitting, where the black and red lines represent the real and imaginary parts, respectively. The virtical green and blue lines represents $\bar{K}N$ threshold and pole position of $\Lambda(1405)$, respectively.

Chapter 2

Experimental setup

Chapter 3

Analysis

Chapter 4

Discussion

4.1 Decomposition of the $K^- d \to n\pi^+\pi^- n$ events

4.1.1 Backward $\pi^\mp\Sigma^\pm$ event selection

4.1.2 Template fitting

4.2 Conversion to the cross section

4.3 Spectra

4.3.1 Qualitative properties of obtained spectra

4.3.2 Comparison with theoritical calculations

4.3.3 $\bar{K}N$ Pole parameters assuming the 2-step reaction

4.3.4 Comparison with DCC model

Chapter 5

Conclusion

Appendix A

$\pi^0\sum^0$ spectrum analysis

Appendix B

Detector resolution

B.1 CDC resolution

B.2 Detector resolution on the $d(K^-, N)$

Appendix C

$d(K^-, n)K^0n$ analysis

Bibliography

[1] R.L. Workman et al. (Particle Data Group), Prog. Theor. Exp. Phys. 2022, 083C01 (2022)
"Review of Particle Physics"

[2] R. H. Dalitz and A. Deloff, J. Phys. G17, 281 (1991).
"The Shape and Parameters of the $\Lambda(1405)$ Resonance"

[3] M. Hassanvand et el., Phys. Rev. C **87**, 055202 (2013)
"Theoretical analysis of $\Lambda(1405) \rightarrow (\pi\Sigma)^0$ mass spectra produced in $p + p \rightarrow p + \Lambda(1405) + p$ reactions"

[4] J. Esmaili, Y. Akaishi, and T. Yamazaki, Phys. Lett. B **686**, 23 (2010)
"Experimental confirmation of the $\Lambda(1405)$ ansatz from resonant formation of a $K^- p$ quasi-bound state in K^- absorption by ^{3}He and ^{4}He"

[5] R. H. Dalitz and S. F. Tuan, Phys. Rev. Lett. 2 (1959).
"Possible Resonant State in Pion-Hyperon Scattering"

[6] M. H. Alston, L. W. Alvarez, P. Eberhard and M. L. Good,
Phys. Rev. Lett. 6, 698 (1961).
"Study of Resonances of the Σ-π System"

[7] R. J. Hemingway, Nucl Phys B **253**, 742 (1985).
"Production of $\Lambda(1405)$ in $K^- p$ Reactions at 4.2GeV/c"

[8] B. Conforto et el., Nucl. Phys. B **34**, 41 (1971).
"New experimental results on the Reactions $K^- p \rightarrow \bar{K}N$ and $K^- p \rightarrow \Sigma\pi$ a partial-wave analysis between 430 and 800MeV/c"

[9] A. J. Van Horn, Nucl. Phys. B **87**, 145 (1975).
"Energy dependent partial-wave analysis of $K^- p \rightarrow \Lambda\pi^0$ between1540 and 2215MeV"

[10] R. J. Hemingway et el., Nucl. Phys. B **91**, 12 (1975).
"New data on $K^-p \to K^-p$ and K^0n and a partial-wave analysis between 1840 and 2234MeV center of mass energy"

[11] P. Baillon and P. J. Litchfield, Nucl. Phys. B **94**, 39 (1975).
"Energy-independent partial-wave analysis of $\bar{K}N \to \Lambda\pi$ between 1540 and 2150 MeV"

[12] G. P. Gopal et al., Nucl. Phys. B **119**, 362 (1977).
"Partial-wave analyses of KN two-body reactions between 1480 and 2170 MeV"

[13] W. E. Humphrey and R. R. Rose, Phys. Rev. **127**, 1305(1962).
"Low-Energy Interactions of K^- Mesons in Hydrogen"

[14] J. K. Kim, Phys. Rev. Lett. **19**, 1074 (1967).
"Multichannel Phase-Shift Analysis of $\bar{K}N$ Interaction in the Region 0 to 550 MeV/c"

[15] A. D. Martin, Nucl. Phys. B **179**, 33 (1981).
"Kaon-Nucleon Parameters"

[16] J. D. Davies et al., Phys. Lett. **83B**, 55 (1979).
"Observation of kaonic hydrogen atom X-rays"

[17] M. Izycki et al., Z. Phys. A 297, 11 (1980).
"Results of the search for K-series X-rays from kaonic hydrogen"

[18] P. M. Bird et al., Nucl. Phys. A **404**, 482 (1983).
"Kaonic Hydrogen atom X-rays"

[19] M. Iwasaki et el., Phys. Rev. Lett. **78**, 3067 (1997).
"Observation of Kaonic Hydrogen K_α X Rays"

[20] M. Bazzi et el., Phys. Lett. B **704**, 113 (2011).
"A New Measuerment of Kaonic Hydrogen X-Rays"

[21] J.C.Nacher et el., Phys. Lett. B **455**, 55 (1999).
"Photoproduction of the $\Lambda(1405)$ on the proton and nuclei"

[22] M. Niiyama et el., Phys. Rev. C **78**, 035202 (2008).
"Photoproduction of $\Lambda(1405)$ and $\Sigma(1385)$ on the proton at E_γ = 1.5-2.4GeV/c"

[23] K. Moria for the CLAS Collaboration,
Phys. Rev. C **87**, 035206 (2013).
"Measurement of the $\pi\Sigma$ photoproduction line shapes near the $\Lambda(1405)$"

[24] K. Moria for the CLAS Collaboration,
Phys. Rev. Lett. **112**, 082004 (2014).
"Spin and parity measurement of the $\Lambda(1405)$ baryon"

[25] S. X. Nakamura, and D. Jido, Prog. Theor. Exp. Phys., 023D01 (2014)
"Lambda (1405) photoproduction based on the chiral unitary model"

[26] D. Jido et el., Nucl. Phys. A **725**, 181 (2003).
"Chiral Dynamics of the Two $\Lambda(1405)$ States"

[27] G. Agakishiev for the HADES Collaboration,
Phys. Rev C **87**, 025201 (2013).
"Baryonic Resonances to the $\bar{K}N$ threshold: The case of $\Lambda(1405)$ in pp collisions"

[28] Y. Ikeda, T. Hyodo, and W. Weise, Nucl. Phys. A **881**, 98 (2012)
"Chiral SU(3) theory of antikaon–nucleon interactions with improved threshold constraints"

[29] Z.-H. Guo and J. Oller, Phys. Rev. C **87**, 3, 035202 (2013)
"Meson-baryon reactions with strangeness -1 within a chiral framework"

[30] M. Mai and U.-G. Meißner, Eur. Phys. J. A **51**, 3, 30 (2015),
"Constraints on the chiral unitary amplitude from $\pi\Sigma K^+$ photoproduction data"

[31] H. Zhang et el., Phys. Rev. C **88**, 035204 (2013).
"Partial-wave analysis of $\bar{K}N$ scattering reactions"

[32] H. Zhang et el., Phys. Rev. C **88**, 035205 (2013).
"Multichannel parametrization of $\bar{K}N$ scattering amplitudes and extraction of resonance parameters"

[33] H. Kamano et el., Phys. Rev. C **90**, 065202 (2014).
"Dynamical Coupled-Channels Model of K^-p Reactions:
Determination ofPpartialWwaveAamplitudes"
Phys. Rev. C**92**, 025205 (2015).
"Dynamical Coupled-Channels Model of K^-p Reactions. II

Extraction of Λ^* and Σ^* Hyperon Resonances"
Phys. ReV. C**95**, 044903(E) (2015).

[34] O. Braun et el., Nucl. Phys. B **129**, 1 (1977).
"New Information About the Kaon-Nucleon-Hyperon Coupling Constants $g(KN\Sigma(1197)), g(KN\Sigma(1385))$ and $g(KN\Lambda(1405))$"

[35] D. Jido, E. Oset and T. Sekihara, Eur. Phys. J. A **42**, 257 (2009).
"Kaonic Production of $\Lambda(1405)$ off deuteron target in chiral dynamics"

[36] J. Yamagata-Sekihara, T. Sekihara, and D. Jido, Prog. Theor. Exp. Phys.**2013**, 043D02 (2013).
"Production of hyperon resonances induced by kaons on a deuteron target"

[37] H. Noumi et el., Proposals for the 15th PAC meeting
"Spectroscopic study of hyperon resonances below $\bar{K}N$ threshold via the (K^-, n) reaction on Deuteron"

[38] K. Miyagawa, J. Haidenbauer, and H. Kamada Phys. Rev. C **97**, 055209 (2018)
"Faddev approach to the reaction $K - d \to \pi\Sigma n$ at $p_K = 1.0GeV/c$"

[39] E. Oset, A. Ramos, and C. Bennhold, Phys. Lett. B **527**, 99 (2002); **530**, 260(E) (2002).
"Low lying $S = -1$ excited baryons and chiral symmetry"

[40] A. Cieplý and J. Smejkal, Nucl. Phys. A **881**, 115 (2012).
"Chirally motivated $\bar{K}N$ amplitudes for in-medium applications"

[41] S. Ohnishi et el, Phys. Rev. C **93**, 025207 (2016).
"Strcture of the $\Lambda(1405)$ and the $K^- d \to \pi\Sigma n$ reaction"

[42] H. Kamano et el., Phys. ReV. C**94**, 065205 (2016).
"Toward Establishing Low-Lying Λ and Σ Hyperon Resonances with the $\bar{K} + d \to \pi + Y + N$ Reaction"

[43] H. Noumi for the E31 Collaboration, Phys. ReV. B**837**, 137637 (2023).
"Pole Position of $\Lambda(1405)$ measured in $d(K^-, n)\pi\Sigma$ reaction"

[44] S. Kawasaki's Doctor thesis will be submitted.

[45] K. Agari et el, Prog. Theor. Exp. Phys., 02B009 (2012)

[46] K. Agari et el, Prog. Theor. Exp. Phys., 02B011 (2012)

[47] TRANSPORT http://linac96.web.cern.ch/Linac96/Proceedings/Thursday/THP72/Paper.pdf

[48] T. K. Ohska et al., Nuclear Science, IEEE Transactions on 33, 98 (1986).

[49] M. Shiozawa and et el., A new TKO system manager board for a dead-time-free data acquisition system, in 1994 IEEE Nuclear Science Symposium-NSS'94, pages 632–635, (1994)

[50] M. Iio et al., Nucl. Instrum. Methods Phys. Res., Sect. **A** 687, 1 (2012).

[51] S. Agostinelli et al., Nucl. Instrum. Methods Phys. Res., Sect. **A** 506, 250 (2003)
J. Allison et el., IEEE Transactions on Phys. Sci. 53, 207 (2006)
J.Allison et al., Nucl. Instrum. Methods Phys. Res., Sect. **A** 835, 186 (2016)

[52] K. Fuji, `https://www-jlc.kek.jp/subg/offl/lib/docs/helix_manip/node3.html` (1968).

[53] Opera Electromagnetic FEA Solution Software

[54] V. Flaminio et al., CERN-HARA-87-01, 121 (1983).

[55] M.Jones et el, Nucl. Phys. B **90**, 349 (1975)

[56] R. Barlow and C. Beeston, Comp. Phys. Comm. **77**, 219 (1993).
"Fitting using finite Monte Carlo samples"

[57] A. Nappi, Comp. Phys. Comm. **180**, 269 (2009).

[58] C.J.S. Damerell et. el., Ncul. Phys. B**129**, 397 (1977). "
K^-n elastic scattering between 610 and 840 MeV/c"

[59] M. jones, R. Levi, Setti, D. Merrill and R. D. Tripp, Phys. Rev. B**90**, 349 (1975). K^-p charge exchange and hyperon production cross section from 860 to 1000 MeV/c

[60] M. Bernheim and et. el., Nucl. Phys. A**365**, 349, (1981). Momentum distributions of nucleons in the deutron from $d(e, e'p)n$ reaction

[61] R. Machleidt, Phys. Rev. C**63**, 024001 (2001).

[62] R. Barlow and C. Beeston, Comp. Phys. Comm. **77**, 219 (1993).

[63] L. Lensniak, AIP Conf. Proc. 1030, 238–243 (2008). New formula for a resonant scattering near an inelastic threshold

[64] S. Agostinelli et al., Nuclear Instruments and Methods in Physics Research Section A: Accelerators, Spectrometers, Detectors and Associated Equipment **506**, 250 (2003).
J.Allison et el., Nuclear Instruments and Methods in Physics Research Section A: Accelerators, Spectrometers, Detectors and Associated Equipment **835**, 186 (2016).